Kovove Mater. 52 2014 269–277
DOI: 10.4149/km_2014_5_269

Assessment of fatigue damage development in power engineering steel by local strain analysis

D. Kukla[1], Z. Kowalewski[1], P. Grzywna[1]*, K. Kubiak[2]

[1]*Institute of Fundamental Technological Research, Polish Academy of Sciences, Pawińskiego 5B, 02-106 Warszaw, Poland*
[2]*Rzeszow University of Technology, Faculty of Mechanical Engineering and Aeronautics, Powstańców Warszawy 8, 35-959 Rzeszow, Poland*

Received 17 December 2012, received in revised form 20 March 2014, accepted 20 March 2014

Abstract

The results of analysis of fatigue damage development in the X10CrMoVNb9-1 (P91) steel specimens subjected to various cyclic loading combinations are presented. The study concerning a quantitative assessment of damage is based on analysis of the fatigue hysteresis evolution in subsequent loading cycles. According to the elaborated algorithms, damage parameters were determined on the basis of two indicators, i.e., average strain and strain amplitude variations. Each of them was responsible for a single damage development mechanism. The average strain characterized ratcheting effect, which is usually related to local generation of plastic strain surrounding microstructural elements. The second damage mechanism called cyclic plasticity is connected with micro slips preceding slip bands formation. The paper also discusses the results of metallographic and fractographic microscopic (SEM) observations of the tested specimens in order to indicate microstructural aspects of fatigue damage development mechanisms.

K e y w o r d s: fatigue test, steels, fracture, scanning electron microscopy, microstructure

1. Introduction

Fatigue degradation testing in a stage preceding crack formation requires registration of strain and stress variation in the gauge length of a specimen during subsequent loading cycles. In our experimental program all fatigue tests were carried out under uniaxial stress state due to symmetrical stress controlled tension-compression cycles on axisymmetric specimens. The study was carried out on samples of the P91 steel applied to the elements of power plants operating under high creep and high fatigue cycles. Under these conditions, there is a degradation of the material, the knowledge of which is essential for the development of new diagnostic methods for measuring the development of the damage and the estimated life of the installation and construction. These methods, based on modern solutions in the area of nondestructive testing and developed by members of the authors team, make it possible to detect subtle structural changes accompanying degradation processes [1–7]. Therefore, understanding the relationship between the degree of degradation of the measured parameters of microstructural deformation and changes may be important to optimize the diagnostic procedures of the NDT area.

It was assumed that mechanical fatigue degradation processes were developing due to an interaction of two types of damage mechanisms: ratcheting, generated by local strain developing around the microstructural inclusions, voids or precipitations being stress concentrators, and cyclic plasticity, associated with slip dislocations on either grain or subgrain scale. In both cases strain variation measured for whole gauge length of the specimen was a sum of local strains developing around defects or local slips in the case of ratcheting or cyclic plasticity, respectively. Cyclic loading caused triggering of various mechanisms of damage initiation and its development depending on material composition, manufacturing technology and loading conditions. In this work, high-cycle fatigue tests were carried out on the P91 steel specimens at various stress amplitudes. The results were correlated with the microstructural observation.

*Corresponding author: tel.: +48 22 826 98 00; e-mail address: pgrzywna@ippt.gov.pl

Table 1. Chemical composition of the P91 steel specimens (results of tests on the scrap of pipeline and recommendations of the Polish Standards)

X10CrMoVNb9-1 (P91)	C	Mn	Cr	Mo	V	Ni	Cu	Si	Al	S	P
Scrap of the pipeline	0.12	0.39	8.31	0.82	0.29	0.18	0.15	0.25	0.025	0.01	
PN 10216-2:2004	0.08–0.12	0.3–0.6	8.0–9.5	0.85–1.1	0.18–0.25	< 0.4	< 0.3	0.2–0.5	< 0.04	< 0.01	< 0.002
PN – EN 10222-2:2002											

Table 2. Mechanical parameters of the P91 steel determined from tests and suggested by the Polish Standards

	R_m (MPa)	R_e (MPa)	A (mm mm^{-1})
According to tensile tests	910	670	0.21
Standard deviation (5 specimens)	9.75	9.88	0.0129
According to Polish Standards: PN 10216-2:2004	630–830	> 450	0.17–0.19

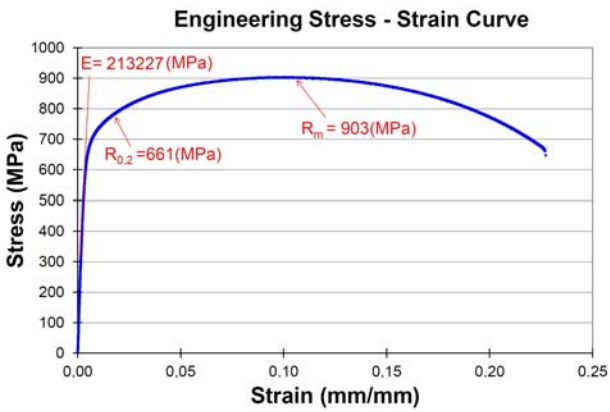

Fig. 1. Tensile stress-strain curve of the P91 steel.

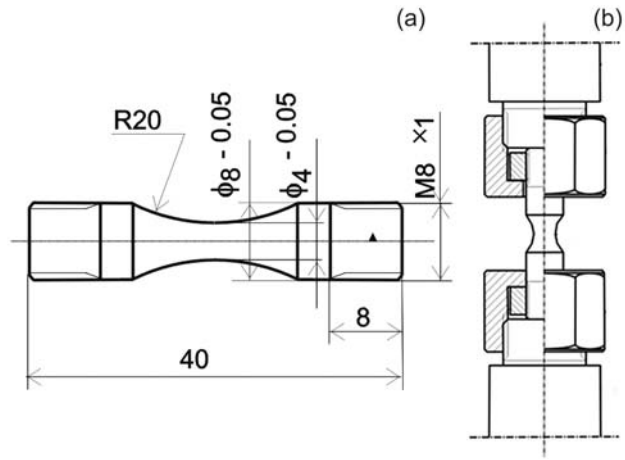

Fig. 2. Specimen (a) and gripping system (b) used for fatigue tests.

2. Material and experimental methodology

All fatigue experiments were carried out on the specimens made up of a material taken from a scrap of a new pipeline made of the X10CrMoVNb9-1 (P91) steel, dedicated to work in real steam conditions. Before testing, the chemical composition of the material was controlled in order to check its agreement with the standard composition. The results shown in Table 1 confirm the compatibility of the chemical composition of the material with the recommendations of the Polish Standards.

2.1. Tension tests

In order to determine mechanical parameters of the P91 steel, the standard static tension tests for 5 specimens were carried out. The representative stress-strain curve from these tests is shown in Fig. 1. On the basis of tensile tests the average mechanical parameters of the P91 steel were determined (Table 2).

2.2. Fatigue tests

Fatigue tests were carried out on hourglass specimens with circular cross section of the diameter in their narrowest place equal to 4 mm (Fig. 2a). A special gripping system enabling specimen to be mounted in the testing machine jaws without any misalignment is shown in Fig. 2b. A transversal extensometer was used to measure a specimen diameter variation during loading cycles.

On the basis of conventional yield point $R_{0.2}$ determined in tension tests, a fatigue loading range was established within the stress amplitude from 400 to 680 MPa. As it had been mentioned earlier all fatigue tests were stress controlled. The average force was assumed to be 0 at each cycle, and moreover, stress amplitude was kept constant. Seventeen specimens were tested under fatigue conditions.

The experimental program enabled identification of fatigue damage development and the standard

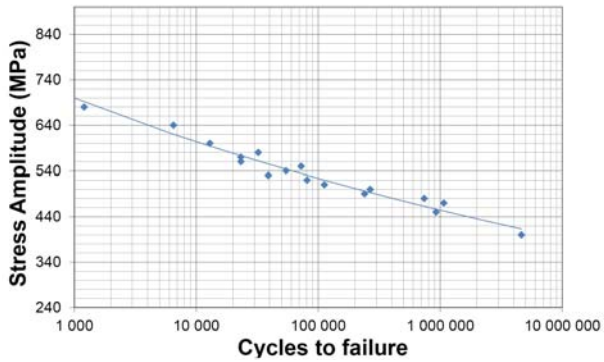

Fig. 3. Wöhler diagram determined for the axisymmetric P91 steel specimens.

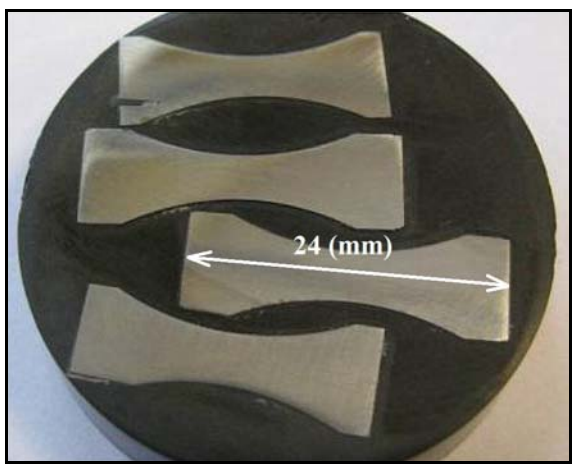

Fig. 4. Metallographic pieces cut from the fatigue specimens along longitudinal cross-section.

Wöhler diagram was determined (Fig. 3).

In order to characterize fatigue damage development, an analysis of strain variations was carried out for selected cycles under various stress amplitudes. Typically materials tested in the high-cycle fatigue range, i.e., stress levels below the yield point of a material in question, exhibit inelastic strain development and durable average strain related to local (due to strain concentration) plastic strain developing around microstructural defects in form of voids, precipitations or nonmetallic inclusions. Therefore, both average strain and strain amplitudes variations were determined as damage indicators for subsequent cycles within a broad range of stress amplitudes.

2.3. Microstructure

After fatigue tests, the metallographic test pieces of longitudinal cross-section were prepared and then subjected to careful analysis (Fig. 4). Two levels of observation were applied, i.e., optical microscopy (OM) and scanning electron microscopy (SEM). The metallographic specimen (dimension ø = 40 mm) which is shown in Fig. 4 was etched with Nital 4 % reagent according to Polish Standards (PN CR 12361:2000).

During the tests with the use of SEM, a chemical composition analysis was carried out in the selected micro-areas using the EDS detector. Among others, a chemical composition assessment of nonmetallic inclusions was identified. Microstructural studies focused on the microstructure and morphology of inclusions visible on metallographic and fractographic samples after fatigue tests. This test had qualitative character, because it did not set quantitative parameters on the basis of stereological calculations.

3. Results

Since the experimental program contained either macroscopic or microscopic investigations of the P91 steel, an attempt had been made to correlate selected parameters characterizing macroscopically fatigue damage development with those coming from microscopic observations. Such approach enables better understanding of phenomena related to damage mechanisms developing during HCF tests.

3.1. Fatigue tests

The fatigue tests carried out in this research indicated that the ratcheting was a dominant mechanism of damage development in the P91 steel. It was responsible for the degradation process in relatively large range of stress amplitudes what can be easily seen in the stress-strain curves of selected cycles carried out at stress amplitudes within 400–600 MPa range.

In the case of the tested steel, two mechanisms of damage development described by change of deformation are defined. In the first mechanism, called cyclic plasticity, an increase of strain amplitude is defined by formula:

$$\varepsilon_{\mathrm{w}} = \frac{\varepsilon_{\max}^{F=0} - \varepsilon_{\min}^{F=0}}{2}, \tag{1}$$

where $\varepsilon_{\max}^{F=0}$ is maximum strain in the cycle and $\varepsilon_{\min}^{F=0}$ is minimum strain in the cycle, what is visible by the change of the hysteresis loop's width.

Another mechanism, ratcheting, is associated with a shift of the hysteresis loop, and thus the average value of the deformation changes, as defined by formula:

$$\varepsilon_{\mathrm{m}} = \frac{\varepsilon_{\max}^{F=0} + \varepsilon_{\min}^{F=0}}{2}, \tag{2}$$

where $\varepsilon_{\max}^{F=0}$ is maximum strain in the cycle and $\varepsilon_{\min}^{F=0}$ is minimum strain in the cycle.

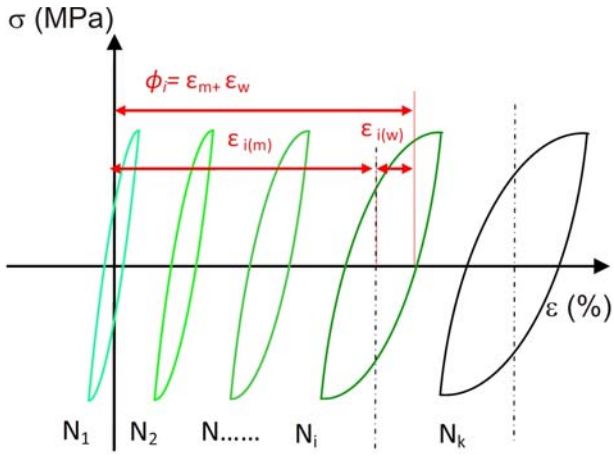

Fig. 5. Scheme of strain development in the consecutive cycles.

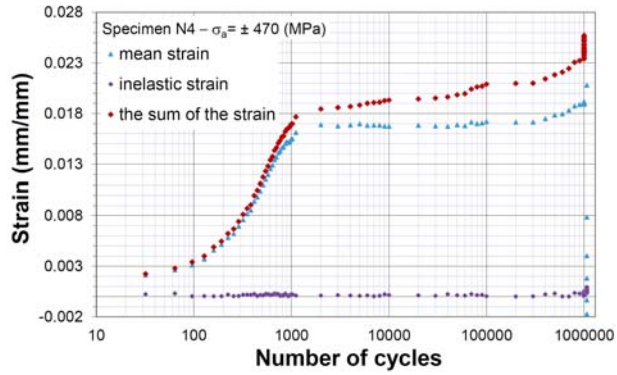

Fig. 7. Strain development within consecutive cycles for stress amplitude of 470 MPa.

Taking into account both mechanisms, a damage indicator ϕ was proposed in the form of sum of the strain amplitude ε_w and mean strain ε_m:

$$\phi = \varepsilon_w + \varepsilon_m. \quad (3)$$

It is graphically explained in Fig. 5.

In the case of specimens tested under cyclic stress amplitude equal to 400 and 470 MPa (Fig. 6a,b), the hysteresis loop width, and as a consequence, the strain amplitude, almost did not change with the consecutive cycles. Contrary to this parameter, the mean level of strain was increasing in the subsequent cycles what was reflected by a shift of the constant-width hysteresis loop with an increase of the number of cycle. Local deformations had a non-symmetrical character when stress direction alternated. This caused that the durable strain in subsequent cycles could increase and decrease (Fig. 6). However, the mechanisms activating a non-symmetrical material response during compression and decompression (in the form of an inclusion debonding from the matrix leading to the formation

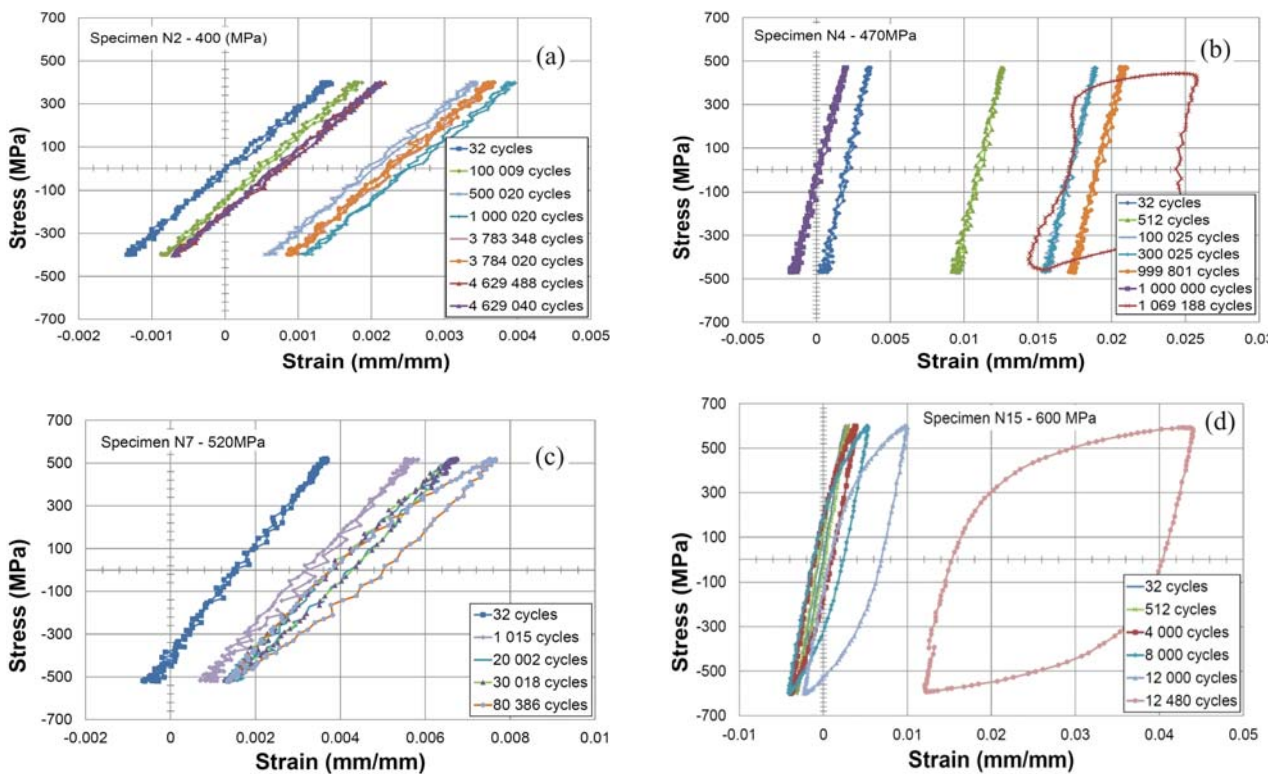

Fig. 6. Hysteresis loop evolution for the stress amplitude of 400 (a), 470 (b), 520 (c) and 600 MPa (d).

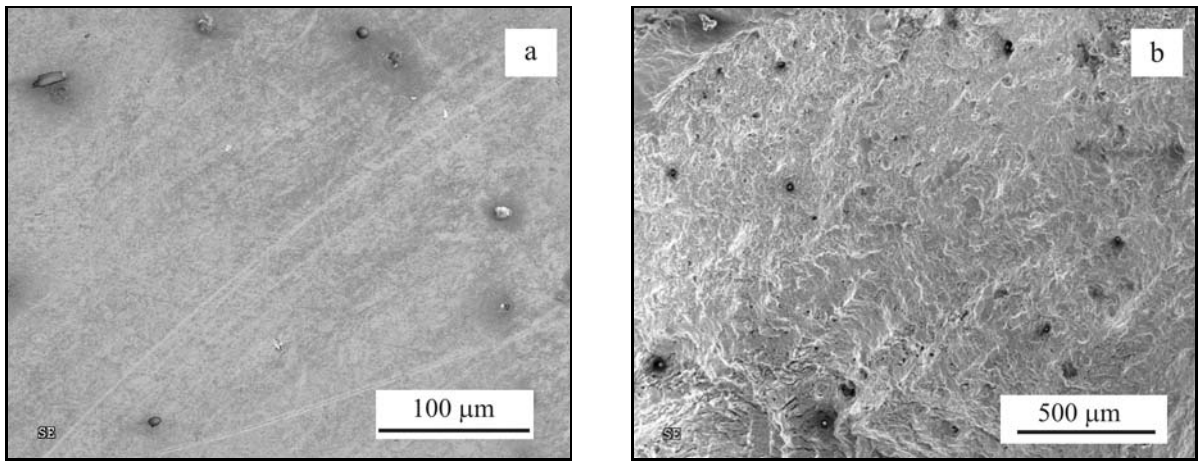

Fig. 8. Microstructure of metallographic test piece (a) and an image of fracture surface (b) of the P91 steel with visible inclusions.

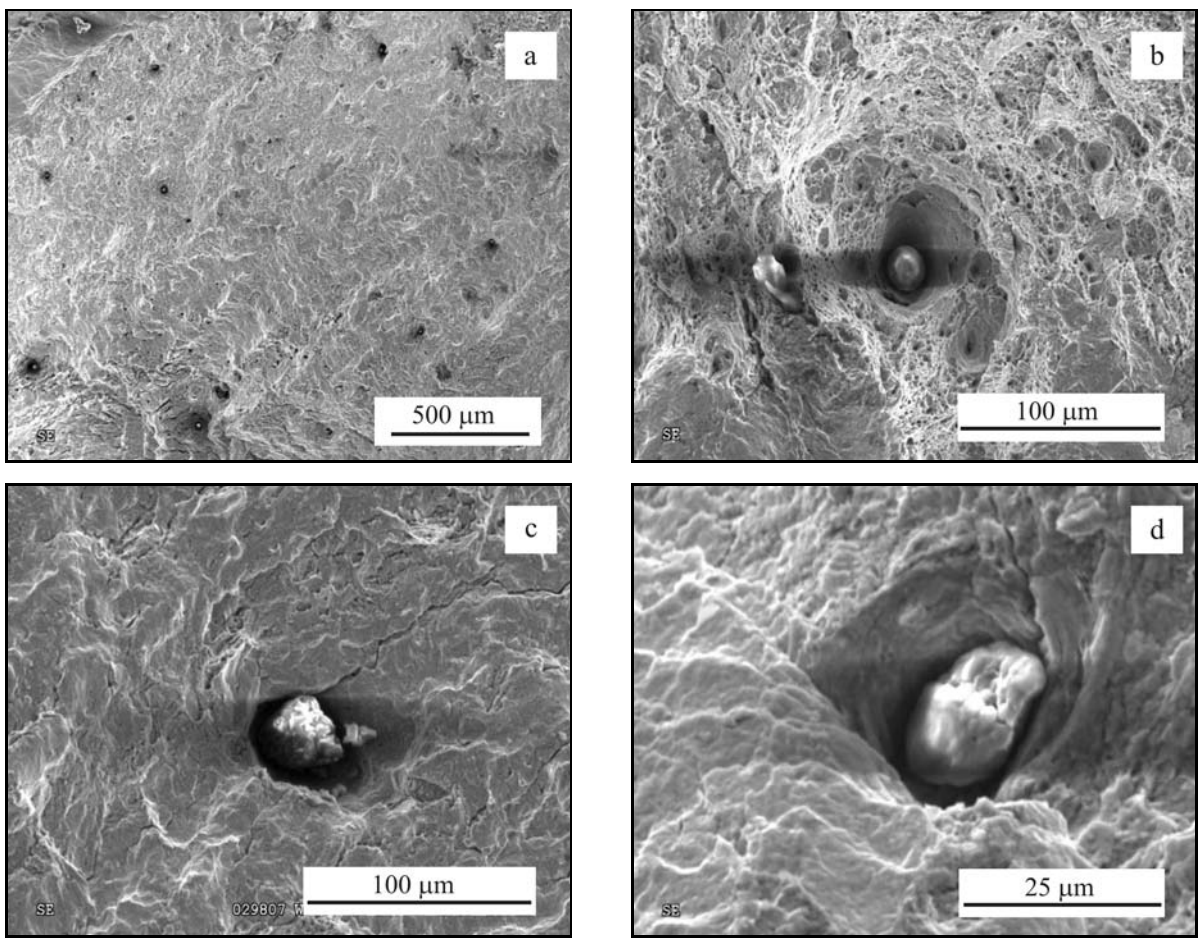

Fig. 9. Non-metallic inclusions of different morphology from final rupture surface shown on the ductile part of fracture (a) and from real fatigue fracture area shown on the brittle part of the surface fracture (b).

of a local strain during tensile stress) usually stimulated an increase of the ratcheting strain until the specimen's decohesion to be attained [7, 8].

In the case of specimens subjected to fatigue tests at higher amplitudes (Fig. 6c,d), one can see an increasing content of the strain amplitude in the total strain distribution during deformation due to cyclic loading. The hysteresis loop in such cases increases its width besides moving along strain axis. For the stress amplitude equal to 600 MPa, the fractions of ratchet-

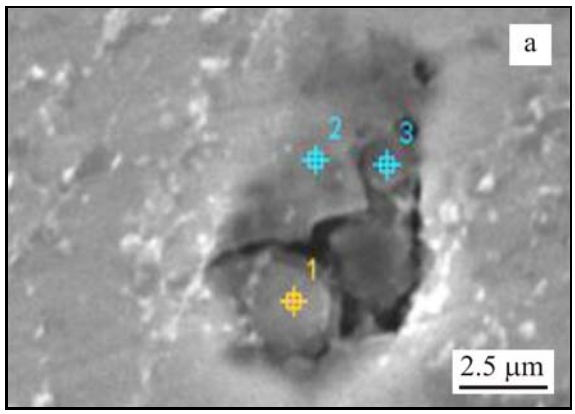

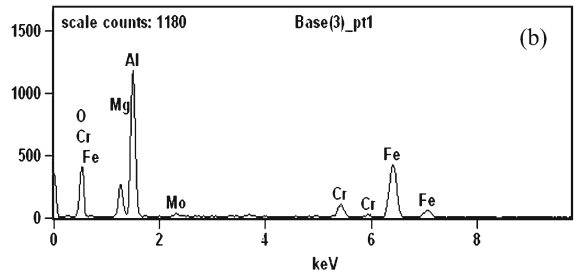

(%)	O-K	Al-K	Cr-K	Fe-K
pt1	60.10	24.52	1.26	7.19

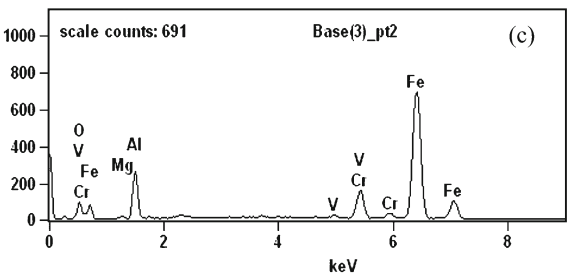

(%)	O-K	Al-K	Cr-K	Fe-K
pt2	36.22	21.86	5.38	34.52

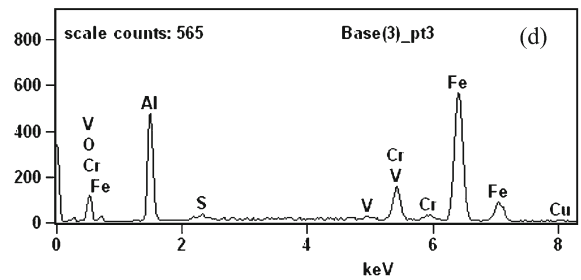

(%)	O-K	Al-K	Cr-K	Fe-K
pt3	43.77	27.83	4.09	22.87

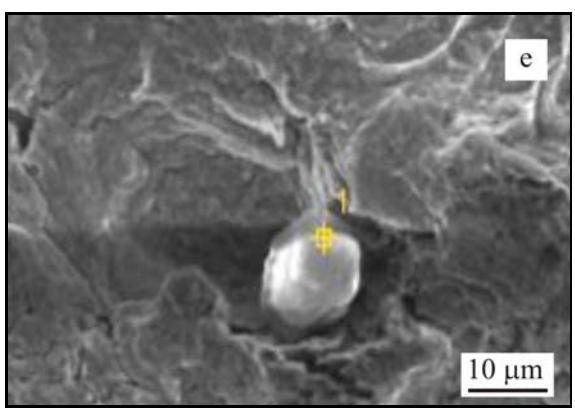

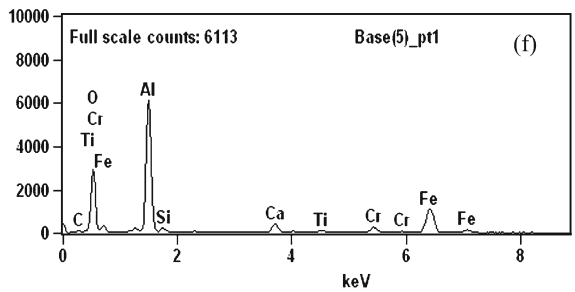

(%)	O-K	Al-K	Cr-K	Fe-K
pt1	45.6	22.3	2.45	16.61

Fig. 10. Inclusions and their weight composition of basic chemical elements. Inclusions in the fatigue zone (a–d). Inclusions in the fatigue fracture surface (e) and (f).

ing and cyclic plasticity are comparable, which leads to an increase of both strain amplitude and durable inelastic strain as well.

On the basis of the evolution of initial fatigue hysteresis loop, the charts of strain development in consecutive cycles were elaborated taking into account the mean level of strain and strain amplitude. A representative chart of this kind is shown in Fig. 7 for stress amplitude of 470 MPa. This figure also reflects the dynamics of strain components sum variation being a parameter enabling the quantitative assessment of fatigue damage extension. Such approach was earlier used (by the authors) to assess fatigue damage development in steel [7, 8] and aluminium alloy [9, 10]. This parameter is defined as a sum of absolute strain values. It enables to cumulate strain components serving as damage indicators independently of their sign.

Based on the diagram shown in Fig. 7 the three phases of damage development can be identified. In the first phase, up to 1000 loading cycles, an increase of strain rate can be observed. The second phase was the longest period characterized by almost linear increase of strain. At the end of it a dominant crack appeared, which started the third phase of damage development. At this period a rapid propagation of the dominant crack was observed leading finally to specimen decohesion. Assessment of fatigue damage mechanisms based on the analysis of material changes in subsequent cycles of deformation has been analyzed

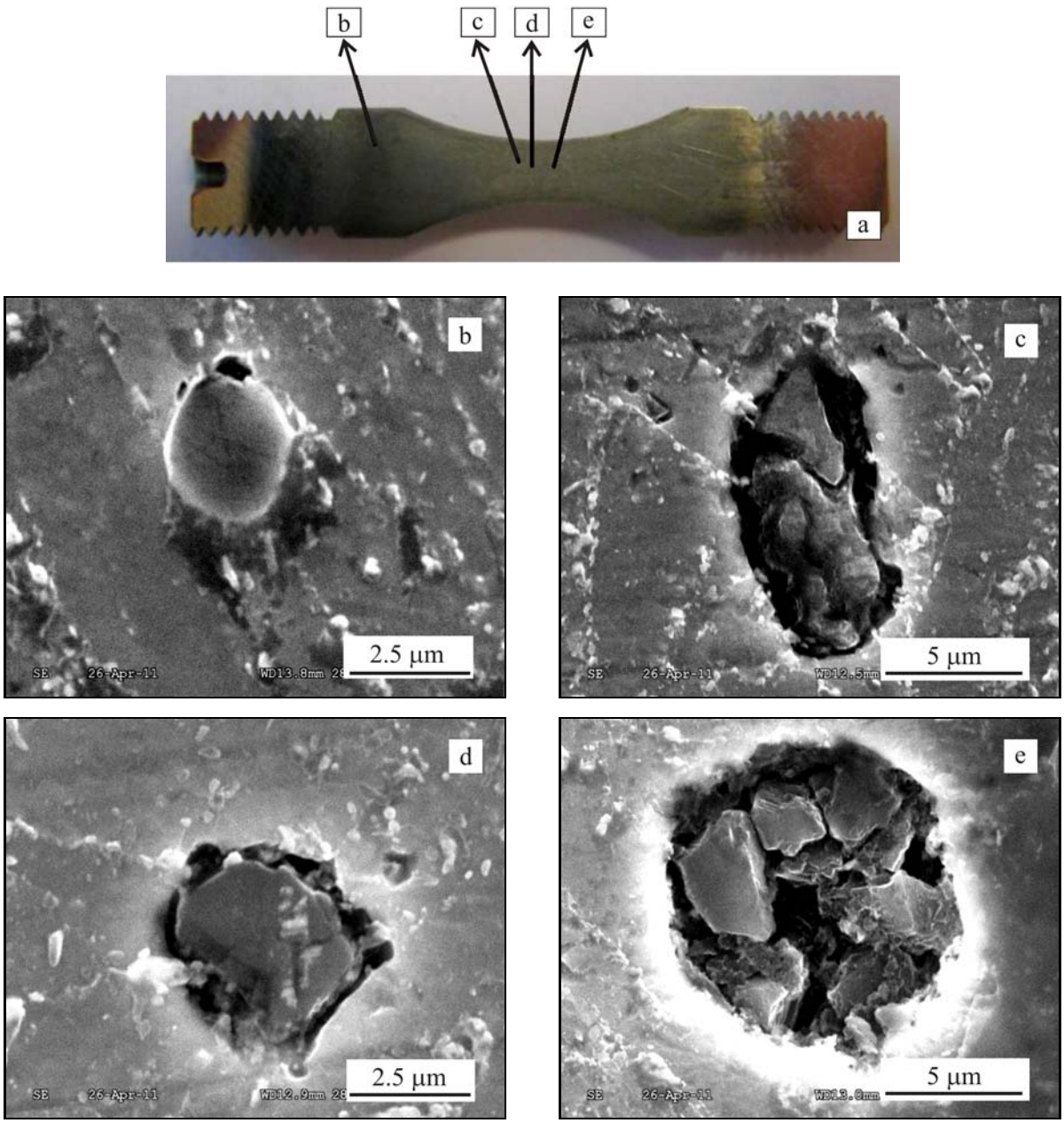

Fig. 11. Longitudinal section of the sample (a) and non-metallic inclusions outside (b) and within (c–e) the zone of fatigue load interaction.

by many research teams either for the P91 steel [11, 12] or other alloys [13, 14].

3.2. Microstructure

Microstructural observations carried out before and after fatigue tests allowed to identify distribution of inclusions well seen on both metallographic test pieces and images of fracture surface of the P91 steel (Fig. 8).

Fractographic investigations revealed the zones of either brittle or quasi-ductile fracture surfaces [17]. Regardless of their character, in all studied fracture surfaces one can notice places of more or less number of inclusions, whose geometry indicates a strongly ceramic character. In this type of steel may be oxides (aluminium, chromium), carbides or nitrides. Examples of such inclusions are presented in Fig. 9. The inclusions shown in Fig. 9a, b are localized on the final rupture surface, where the fracture is more ductile. The particles shown in Fig. 9c, d come from real fatigue fracture area, where the character of fracture is brittle and the microcracks are visible on the inclusions. This fact indicates stress concentrations in these areas, which could affect the morphology of inclusions.

In order to confirm the assumptions related to

the type of inclusions, chemical composition investigations were carried out for selected inclusions located either at fatigue fracture surfaces or at metallographic test pieces. The results of the analysis with marked spots are presented in Fig. 10. The tests have highlighted a comparatively high fraction of oxygen and aluminium, what means that the observed inclusions are aluminium oxides. It was additionally confirmed by the phase contrast and "glare" effect of the non-conductive inclusions. Oxide inclusions observed are the result of the binding of oxygen by the aluminium, which is added to all types of steels as a deoxidizer. Oxides, as hard and brittle ceramic inclusions, are stress concentrators, and the result of cyclic loading is decohesion.

Microstructural investigations also included an observation of longitudinal cross-sections of metallographic specimens after cyclic fatigue loading in a range of significant number of cycles, for which the tests were interrupted before the main crack propagation. For one of the HCF specimens tested at stress level equal to 400 MPa, significant damage of inclusions can be observed independently of their location within specimen. As it is seen in Fig. 11, more plastic metallic matrix surrounding hard inclusions was detached and the inclusions were disintegrated. An image of the inclusion well integrated with the matrix and coming from a grip area of the specimen is presented for comparison. It indicates the existence of microstructural areas surrounding the defects of different morphology. It confirms also the domination of the ratcheting mechanism of damage development under fatigue loading related to local strains.

Microstructural aspects of fatigue damage associated with the development of local deformations around the elements of the microstructure were presented in [15, 16].

4. Conclusions

The paper was devoted to fatigue degradation assessment by means of damage mechanisms identification. The results of macroscopic fatigue tests and microstructural observations enabled to recognize the ratcheting mechanism as dominant during fatigue of the P91 steel. Microstructural tests of the specimens carried out after fatigue tests enabled to identify the matrix deformation surrounding hard ceramic inclusions and debonding process of the inclusions leading to their separation with respect to the matrix. Thus, an influence of microstructural defects different from the matrix properties on the fatigue damage mechanism development was revealed.

A formation of the local micro-discontinuities around inclusions due to cyclic loading leads to conclusion that this kind of defects can influence the strength resistance variation of degraded zones. It can be further analyzed using nondestructive testing methods like eddy currents method or other diagnostic techniques based on either magnetic or ultrasonic parameters variation. This kind of work was conducted in the past and still is developing by other research workers [1–10, 17–20].

Acknowledgement

The research was carried out within the framework of the research project No. N N507 329536.

References

[1] Kowalewski, Z. L., Szelążek, J., Mackiewicz, S., Pietrzak, K., Augustyniak, B.: International Journal of Modern Physics B, *22*, 2008, p. 5533. doi:10.1142/S0217979208050772
[2] Kowalewski, Z. L., Szymczak, T., Makowska, K., Augustyniak, B.: Key Engineering Materials, *488*, 2012, p. 315.
[3] Augustyniak, B., Chmielewski, M., Piotrowski, L., Kowalewski, Z. L.: IEEE Transaction on Magnetics, *44*, 2008, p. 3273. doi:10.1109/TMAG.2008.2002525
[4] Kukla, D., Grzywna, P., Zagórski, A.: Welding Technology Review, *13*, 2012, p. 8. (in Polish)
[5] Żurek, Z. H., Kukla D., Kurzydlowski, K. J.: Review of Electrical Engineering (Przegląd Elektrotechniczny), *7*, 2012, p. 218. (in Polish)
[6] Dietrich, L., Grzywna, P., Kukla, D.: Welding Technology Review, *13*, 2012, p. 81. (in Polish)
[7] Kowalewski, Z., Dietrich, L., Kukla, D., Grzywna, P., Szymczak, T.: Energetics (Energetyka), *65*, 2012, p. 706. (in Polish)
[8] Kukla, D., Grzywna, P.: Energetics (Energetyka), *8*, 2012, p. 436. (in Polish)
[9] Kukla, D., Grzywna, P., Dietrich, L.: In: Proceedings of 28th Danubia-Adria-Symposium on Advances in Experimental Mechanics. Eds.: Ódor, I., Borbás, L. Budapest, GTE 2011, p. 61. ISBN 978-963-9058-32-3
[10] Szymczak, T., Kowalewski, Z. L., Dietrich, L.: Materials Research Innovations, *15*, 2011, p. 53. doi:10.1179/143307511X12858956846913
[11] Polak, J., Petrenec, M., Man, J.: Kovove Mater., *49*, 2011, p. 347.
[12] Narasimhachary, S. B., Saxena, A.: International Journal of Fatigue, *56*, 2013, p. 106. doi:10.1016/j.ijfatigue.2013.07.006
[13] Kunz, L., Lukas, P., Mintach, R., Hrbacek, K.: Kovove Mater., *44*, 2006, p. 275.
[14] Novy, F., Palcek, P., Chalupova, M.: Kovove Mater., *43*, 2005, p. 447.
[15] Karlik, M., Kubosova, A., Hausild, P., Prahl, J.: Kovove Mater., *46*, 2007, p. 77.
[16] Faltus, J., Siegl, J.: Kovove Mater., *45*, 2007, p. 59.
[17] Kukla, D., Dietrich, L., Ciesielski, M.: Acta Mechanica et Automatica, *5*, 2011, p. 55. (in Polish)
[18] Holzwarth, U., Schaaff, P.: Journal of Materials Science, *42*, 2007, p. 5620. doi:10.1007/s10853-006-0993-8

[19] Helifa, B., Oulhadj, A., Benbelghit, A., Lefkaier, I. K., Boubenider, F., Boutassouna, D.: NDT & E International, *39*, 2006, p. 384. doi:10.1016/j.ndteint.2005.11.004

[20] Lee, S. S., Oh, Y. J, Nam, S. W.: Korean Journal of Metals and Materials, *49*, 2011, p. 924.